A Cancellation Method of Periodic Interference in Pulse-Like Signals Using an Adaptive Filter and Its Application to Flash ERGs

Naohiro Toda

Abstract— **This paper proposes a method that uses an adaptive filter to cancel out the periodic interference that appears in transient pulsed signals (this is referred to as a pulse-like signal). Vibrational components that disturb such pulse-like signals, even in the absence of periodic interference, as the signals are input to an adaptive filter were first clarified theoretically. Such components become smaller as the adaptation time of the algorithm is increased. However, when the number of synchronous addition averaging operations is larger, there is a danger of the error (amount of noise) becoming larger than when no adaptive filter is used, because the phase of the periodic interference is locked with respect to the pulse-like signals. This component is referred to as the self-canceling component in this paper. In addition, a mask process is proposed that does not update the adaptive filter coefficient while the pulse-like signals are sustained, with the assumption that the characteristics of the periodic interference do not change rapidly. The ability of this process to inhibit the generation of self-canceling components was verified through a numerical simulation. Furthermore, an adaptive filter that implemented the proposed mask processing was applied to an actual electroretinogram (ERG) with flash light stimuli, and its effectiveness was verified.**

Index Terms— **periodic interference, adaptive filter, RLS algorithm, mask process, electroretinogram (ERG)**

1. Introduction

PERIODIC interference (also referred to as hum noise), which originates from commercial alternating-current (commonly referred as to AC) power sources (50/60[Hz]) or rotating machines, frequently disturbs the measurement of small signals and causes problems. This issue is particularly critical when measuring bioelectric signals such as electroencephalogram (EEG) electrocardiogram (ECG), and electromyogram (EMG), with electrodes fitted on the surface of the human body [1], [2].

An electroretinogram (ERG) records the action potential with respect to light stimulation in the retina [3]. Although the ERG is an objective index of visual function, there are cases where the periodic interference included in the signal presents a significant hindrance, because the response electric potential is minute and includes the fundamental frequencies (50/60[Hz]) of commercial AC power sources and its several harmonic waves in the frequency range [4].

This article published in IEICE Transactions on information and systems Japanese Edition (Vol.J94-D, No. 10, October 2011, pp. 1685-1695, http://www.ieice.org/jpn/books/transaction.html) is translated into English by the author privately.

Author is with the Department of Information Science and Technology, Aichi Prefectural University, Nagakute, Aichi, Japan.

Because such external noises, as represented by periodic interference, manifest themselves at practically the almost same frequency and phase (common mode), a differential amplifier circuit for instrumentation, with a high common-mode rejection ratio (CMRR), is typically used for measuring bioelectric signals [1]. The incidence of common potential, occurring with periodic interference induced at the positive and negative inputs, becomes less frequent in some cases, depending on the nonuniformity of attachment impedances at individual electrodes, the conditions of the body's interiors, and the measurement environment. In some cases, such differences are amplified and retained as significant noise, which requires meticulous cleansing of the skin and improvement of the surrounding environment [2]. However, these responses can often be difficult to achieve at medical sites owing to time and space constraints.

There are many procedures associated with ordinary ERG tests that involve a contact-lens-type electrode fitted over the cornea, such as the administration of anesthetic eye drops in the eye. This can significantly burden both the test subject and the physician. The possibility of fitting a skin electrode to the lower eyelid is therefore being considered [5]. However, skin electrodes offer a poor signal-to-noise (S/N) ratio, making them unsuitable for clinical applications such as local ERG tests [6]. If there was a method to sufficiently cancel periodic interference, then it would be possible to perform ERG tests, using skin electrodes, on patients who are considered difficult subjects for administration (including infants and patients who have just operated on) owing to the impact on the cornea.

The notch filter is commonly used to cancel such periodic interference, but although this filter cancels components of specific frequencies, it also distorts signals whose accurate recording is desired (desired signals). For that reason, the notch filter has been deemed unsuitable for use in ERG testing [4]. Because the frequencies and amplitudes of periodic interference fluctuate and are not constant, it is necessary to track such changes. Methods involving analog circuits [7] and the fitting method [8] (involving nonlinear optimization of a sinusoidal wave model for measured data over a short period of time) have been proposed for estimating frequencies, phases, and amplitudes of periodic interference in individual signal measurements. However, there remain issues on real-time implementation or treatment of higher harmonic waves. Real-time noise cancellation is desirable for ERG tests conducted by a physician, who would perform such tests while verifying responses from the tested eye.

Adaptive filters that are driven by algorithms, such as least mean squares (LMS) [9],[10] and recursive least squares (RLS) [11], are potential methods for responding to such needs, but so far no detailed investigations have been conducted on measuring transient signals that rapidly change at a particular time but then gradually decrease to 0, such as the pulse-like signal of the ERG.

In this paper, we deduce theoretically that the adaptive filter generates components that disturb the desired signal owing to the existence of the desired signal itself, based on the successive least squares method, which is a common framework that includes the LMS and RLS algorithms for an adaptive filter. A serious problem that occurs when the desired signal is a pulse-like signal will also be pointed out: the components that work to negate the existence of the desired signal are manifested as clear vibrating components similar to periodic interference. Such vibrational components cannot be reduced by the synchronous addition averaging process.

Furthermore, we propose a mask process that does not update the filter coefficient during the interval in which the pulse-like signal is considered to be manifest. Using numerical simulations, we will show that the cancellation of periodic interference can be achieved without generating such vibrational components, which are referred to as the self-canceling components defined in section 2. In order to demonstrate its effectiveness, the mask process is applied to an actual flash light ERG.

2. Cancellation of periodic interference with adaptive filter and associated problems

2.1 Periodic interference and adaptive filter

Let us consider a periodic interference $u(k)$, whose frequencies and amplitudes within a time interval of up to a certain length can be considered to be constants, as

$$u(k) = \sum_{i=0}^{m} A_i \cos\left(2\pi(i+1)\frac{f_0}{f_s}k + \phi_i\right) \tag{1}$$

where f_0[Hz] is a fundamental frequency of the periodic interference, and m is the number of higher harmonic waves. Furthermore, the signals, including $u(k)$, treated in this paper are sampled at f_s[Hz] and have discrete time $k \in \{0, \pm1, \pm2, \cdots\}$.

If an appropriate analog process is implemented, and no aliasing occurs, we should have $m \leq \lfloor \frac{f_s}{2f_0} \rfloor - 1$. Furthermore, A_i and ϕ_i are, respectively, the ith amplitude and phase of the ith higher harmonic wave, and are expressed as $0 \leq A_i, -\pi \leq \phi_i < \pi$.

On the other hand, let us consider the desired signal to be $s(k)$. If the periodic interference, with varying amplitude and phase

$$n_{ac}(k) = \sum_{i=0}^{m} G_i \cos\left(2\pi(i+1)\frac{f_0}{f_s}k + \theta_i\right), \tag{2}$$
$$(0 \leq G_i, -\pi \leq \theta_i < \pi)$$

is added, then the measured signal would be

$$d(k) = s(k) + n_{ac}(k). \tag{3}$$

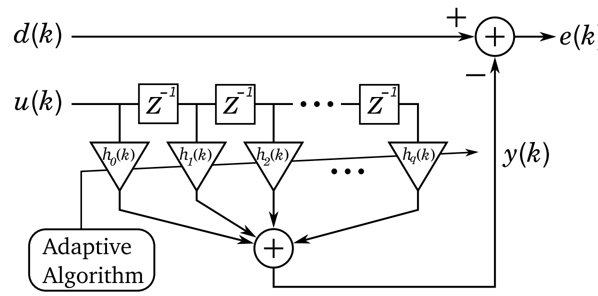

Fig. 1. Interference cancelling with adaptive filter

The cancellation of the periodic interference is expressed by letting the second term on the right-hand side of Equation (3) be 0. The signal, as given by Equation (1), is employed as the reference signal. On the other hand, if we apply the qth-order finite impulse response (FIR) filter with the time-varying coefficients $h_\ell(k), (\ell \in \{0, 1, \cdots, q\})$, we get

$$y(k) = \sum_{\ell=0}^{q} h_\ell(k) u(k-\ell). \tag{4}$$

Then, the residual signal is obtained by subtracting the output $y(k)$ of the filter above from the main input $d(k)$ given as the measurement signal:

$$e(k) = d(k) - y(k). \tag{5}$$

Assuming that the discrete Fourier transform (frequency transfer function) of $h_\ell(k)$

$$H(k, \varphi) = \sum_{\ell=0}^{q} h_\ell(k) \exp\left(-j2\pi\frac{\varphi}{f_s}\ell\right), \tag{6}$$

where j is considered an imaginary unit, satisfies the following relationship for all of $p \in \{0, 1, \cdots, m\}$:

$$\begin{cases} |H(k, f_0 \cdot (p+1))| &= \dfrac{G_p}{A_p} \\ \angle H(k, f_0 \cdot (p+1)) &= \theta_p - \phi_p \ , \end{cases} \tag{7}$$

we can then state

$$e(k) = s(k). \tag{8}$$

The residual signals will be only the desired signal, and the periodic interference would be completely canceled. For this to occur, two coefficients are required for each sinusoidal wave. Hence, the filter order q must be

$$2m + 1 \leq q. \tag{9}$$

Furthermore, it is necessary to determine the value of the filter coefficient in order to satisfy Equation (7). A system that depends on the properties of the input signals and performs processes with varying filter coefficients successively is ordinarily referred to as an adaptive filter [11]. The concept of noise cancellation using such a system is shown in Figure 1. The determination of coefficients based on the successive least squares method is described below. Because $n_{ac}(k)$ and

$y(k)$ are derived by linearly filtering the reference signal $u(k)$, if we assume that

$$v(k) = n_{ac}(k) - y(k), \tag{10}$$

then, based on Equations (3) and (5), we get

$$e(k) = s(k) + v(k). \tag{11}$$

The weight sequence $w(i)$ $(i \in \{0, 1, 2, \cdots\})$, which decays with index i is applied to the sum of squares of the error to the present point in time:

$$\begin{aligned} J(k) &= \sum_{i=0}^{\infty} w(i)e^2(k-i) \\ &= \sum_{i=0}^{\infty} w(i)\big(s^2(k-i) + v^2(k-i) \\ &\qquad + 2s(k-i)v(k-i)\big). \end{aligned} \tag{12}$$

The effective length of $w(i)$ is equivalent to the adaptation time of the filter. If the third term on the right side is sufficiently small, in other words, if the correlation between the desired signal $s(k)$ and $v(k)$ [$v(k)$ is a linearly filtered signal of the reference signal $u(k)$] can be ignored then we get

$$\begin{aligned} J(k) = \sum_{i=0}^{\infty} w(i)e^2(k-i) = \sum_{i=0}^{\infty} w(i)s^2(k-i) \\ + \sum_{i=0}^{\infty} w(i)\big(e(k-i) - s(k-i)\big)^2 \end{aligned} \tag{13}$$

[12]. Because the first term on the right-hand side does not depend on the filter coefficient, Equation (8) is expected to hold by minimizing the left-hand side. In order to minimize $J(k)$, we use a condition for the partial differentiation to each filter coefficient:

$$\frac{\partial J(k)}{\partial h_\ell(k)} = 0. \tag{14}$$

These coefficients can be successively solved as shown in Equation (15):

$$\boldsymbol{h}_k = \boldsymbol{R}_k^{-1} \boldsymbol{z}_k, \tag{15}$$

where $\boldsymbol{R}_k$ is a symmetric $(q+1) \times (q+1)$ autocorrelation matrix of $u(k)$ having elements at the ℓth row and the nth column $(\ell, n \in \{0, 1, \cdots, q\})$:

$$r_{\ell,n}(k) = \sum_{i=0}^{\infty} w(i)u(k-i-\ell)u(k-i-n). \tag{16}$$

Furthermore, the filter coefficient $\boldsymbol{h}_k$ and the cross-correlations $\boldsymbol{z}_k$ between $d(k)$ and $u(k)$ are

$$\boldsymbol{h}_k = (h_0(k)\ h_1(k)\ \cdots\ h_q(k))^t, \tag{17}$$

$$\boldsymbol{z}_k = (z_0(k)\ z_1(k)\ \cdots\ z_q(k))^t, \tag{18}$$

$$\text{where} \quad z_\ell(k) = \sum_{i=0}^{\infty} w(i)d(k-i)u(k-i-\ell), \tag{19}$$

respectively, and $(\cdot)^t$ indicates transposition.

The infinite sums in Equations (16) and (19) are regarded as a form of convolution between the weight $w(k)$ and signals formed from products of $d(k)$ and $u(k)$. Consequently, we can execute successive determinations of $\boldsymbol{h}_k$ with finite operations. For instance, in considering

$$w(i) = \lambda^i, \quad 0 < \lambda < 1 \tag{20}$$

the effects of the past are reduced exponentially, but $r_{\ell,n}(k)$ of Equation (16), and $z_\ell(k)$ of Equation (19) can be easily expressed as, respectively,

$$r_{\ell,n}(k) = \lambda r_{\ell,n}(k-1) + u(k-\ell)u(k-n), \tag{21}$$

and

$$z_\ell(k) = \lambda z_\ell(k-1) + d(k)u(k-\ell), \tag{22}$$

with an infinite impulse response (IIR) filter of the first degree.

The RLS algorithm [11] uses Equation (20) as $w(i)$ and is an accelerated version of the successive least squares method expressed by Equation (15) via the inverse matrix theorem. λ is referred to as the forgetting factor.

Furthermore, by letting

$$w(i) = \delta(i) \tag{23}$$

$$\text{where, } \delta(i) = \begin{cases} 1 & (i = 0) \\ 0 & (i \neq 0) \end{cases}, \tag{24}$$

and then introducing the step size parameters based on the steepest descent principle, we can derive the LMS algorithm [9],[10].

Because this paper discusses the fundamental properties of the adaptive filter, we use Equations (15) and (20) as a basic adaptive algorithm, namely the successive least squares method with a forgetting factor. This method is equivalent to the RLS algorithm.

2.2 *Self-canceling components*

It was described in the previous section that periodic interference can be canceled by minimizing the sum of squares of the error, using the hypothesis that there is no correlation between $u(k)$ and $s(k)$. In actual situations, however, $w(i)$ does not have an infinite length but a finite length or a rapidly decreasing sequence, in order to ensure adaptability. Owing to this finiteness of the analysis period, even if there is no cross-talk from the reference channel to the main input channel [12] and they are essentially uncorrelated, the components of $u(k)$ are observed in $s(k)$. Because the adaptive algorithm works to cancel the components of the reference signal observed in the main signal, the algorithm may cause problems by generating components that cancel the desired signal itself.

In this section, we present an example of the numerical simulation of the problem that occurs during cancellation of the periodic interference included in the pulse-like signals and treat it theoretically.

The sampling frequency is set to $f_s = 1253$[Hz], and the exponential weight and several sinusoidal waves are combined to form a pulse-like signal $s(k)$. Figure 2(a) shows this numerically configured signal indicated as a “true signal” beside the graph. On the other hand, a numerical sample

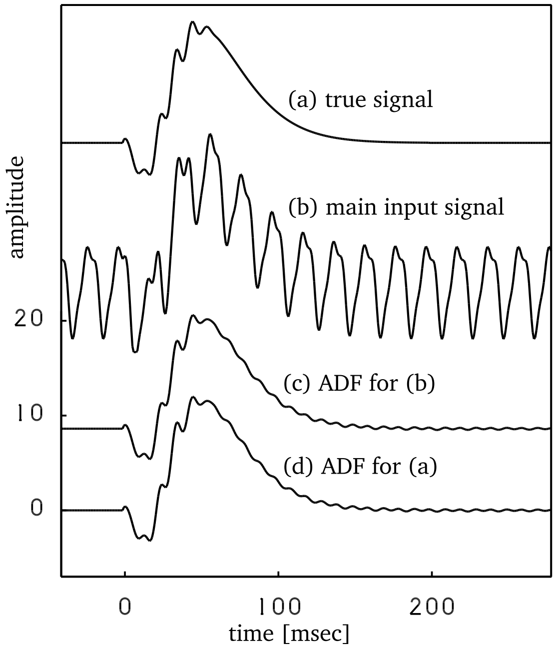

Fig. 2. An example of simulation for periodic interference cancellation of a pulse-like signal using the adaptive filter.

of the periodic interference is configured with sinusoids of fundamental frequency 50[Hz] and its higher harmonics. We configured the main input signal $d(k)$ by adding the true signal configured above and this periodic interference. Figure 2(b) shows the "main input signal". Furthermore, a reference input $u(k)$ that contains harmonic components below 600[Hs]($m = 11$) with an equal amplitude is also configured.

Applying $u(k)$ and $d(k)$ as inputs to an adaptive filter given by Equation (15), we executed the periodic interference cancellation. Figure 2(c) shows the resulting wave form. The adaptive algorithm has an exponential weight expressed by Equation (20) ($\lambda = 0.996$) as $w(i)$. In the figure, the term *adaptive filter* is abbreviated as ADF. The filter order was set to $q = 23$, in accordance with Equation (9). Furthermore, a sufficient period was set for adapting the filter before the pulse-like signal began.

Although periodic interference of larger amplitudes was canceled and the effects thereof were considered significant, the smaller-amplitude vibration components were confirmed in the second half of the pulse-like signal. These vibration components may be considered as residual components due to an excessively large periodic interference. However, because an exactly identical vibration is confirmed as a result (d) of operating an adaptive filter without adding the periodic interference to the waveform of (a), this should be understood as not being a residue of periodic interference. The attempt to cancel periodic interference by using an adaptive filter led to the contrary result of added periodic interference.

In the following, such vibration components are treated theoretically. For the sake of simplicity, we consider the case of periodic interference that has only the fundamental frequency component. That is, by setting m to 0 in the reference signal of Equation (1), $u(k)$ is given by the following Equation (25):

$$u(k) = \cos(fk) \tag{25}$$

where $f = 2\pi \dfrac{f_0}{f_s}$, and $f \neq \ell\pi$, ($\ell \in \{0, \pm1, \pm2, \cdots\}$). Furthermore, in order to observe the influence of $s(k)$ alone, assuming that no periodic interference exists, we get

$$d(k) = s(k). \tag{26}$$

That is, we treat the case shown in Figure 2(d). In such a case, the FIR filter of the conditional Equation (9) regarding the filter order with $q = 1$ (number of coefficents is 2) should be used. If λ is set sufficiently close to 1, Equation (4), which gives the filter output, can be approximated by

$$\widetilde{y}(k) = \sum_{\tau=0}^{\infty} s(\tau) 2(1-\lambda)\lambda^{k-\tau} \cos(f(k-\tau)). \tag{27}$$

The outline of this derivation is shown in the Appendix. Equation (27) is the output of a constant coefficient linear filter having an impulse response of

$$\eta(k) = 2(1-\lambda)\lambda^k \cos(fk). \tag{28}$$

Equation (28) is a cosine wave whose amplitude is decreasing exponentially. Because the amplitude is multiplied by $(1-\lambda)$, it becomes smaller while the response time of the filter becomes longer as λ approaches 1. This means that even when the periodic interference $n_{ac}(k)$ in the measurement signal $d(k)$ is 0, if $s(k)$ is a pulse-like signal like the ERG, the damped vibration waveform that has a periodic interference frequency ends up being added to the residue $e(k)$. Furthermore, because Equation (27) is a convolution operation, when a pulse-like signal is applied, the cosine wave that has its phase locked at the point where the pulse-like signal starts as the origin is subtracted, regardless of the phase of the periodic interference in the reference signal. For that reason, in principle, such components cannot be reduced by using the synchronous addition averaging process. This indicates that if the number of synchronous addition averaging operations is increased, then using the periodic interference cancellation process via an adaptive filter could magnify the error more than when no adaptive filter is used. In this paper, this is referred to as self-canceling components, because Equation (28) depends on the existence of $s(k)$ itself.

The transfer function $G(z)$ from $s(k)$ to $e(k)$ is expressed as

$$\begin{aligned} G(z) &= \frac{S(z) - \widetilde{Y}(z)}{S(z)} \\ &= 1 - \frac{2(1-\lambda)(1-\lambda z^{-1}\cos f)}{1 - 2\lambda z^{-1}\cos f + \lambda^2 z^{-2}}, \end{aligned} \tag{29}$$

where $S(z)$ and $\widetilde{Y}(z)$ are Z-transforms of $s(k)$ and $\widetilde{y}(k)$, respectively. This signifies that it is a notch filter. Similar analyses [10], [13], [14] have been performed with the LMS algorithm when the main input is a stochastic noise. These results are referred to as the non-Wiener solution. However, we found no discussion on cases of the RLS algorithm, or its equivalent algorithm given by Equation (15). Furthermore, the vibration components that significantly manifest themselves immediately following the QRS complex, while canceling periodic interference in electrocardiograms, have been known empirically using methods other than the adaptive filter [15], [16], [17]. However, this has not been dealt with analytically.

3. Mask process

The self-canceling components expressed by Equation (27) become smaller as λ approaches 1 (i.e., as the adaptation time becomes longer). It would be necessary to set the adaptation time from a few seconds to a little over 10[s], because there are fluctuations in the frequencies of periodic interference. In addition, we must consider that the fitting conditions of electrodes vary owing to blinking or eye movements of the test subjects during actual ERG tests and when tests are speeded up. Under such circumstances, the self-canceling components are believed to reach such significant magnitudes that they cannot be ignored.

The self-canceling components occur because individual correlations of Equation (15) are updated in the interval where $s(k)$ rapidly changes. When the length of such an interval is sufficiently short with respect to the degree of change in the properties of the periodic interference, and if the main component of $d(k)$ up to immediately before the start of the pulse-like signal is $n_{ac}(k)$, and if the filter coefficient is such that the periodic interference can be canceled in an ideal manner, then by preventing the updating of correlation in such an interval, it should be possible to prevent the occurrence of self-canceling components.

The mask process for not updating the correlations and filter coefficients, while continuing with the operation of the filter while the pulse-like signal is sustained, is therefore proposed to operate in the following manner:

The mask length is set to M[sample], and the starting time of the pulse-like signal is $\{\tau_1, \tau_2, \cdots, \tau_{N_p}\}$. The intervals between respective time points are sufficiently large in comparison to M. While in the mask interval, that is, if k satisfies $\tau_i \le k \le \tau_i + M$ where $0 \le i \le N_p$, $r_{\ell,n}(k)$ and $z_\ell(k)$ of Equation (15) are not updated as

$$r_{\ell,n}(k) = r_{\ell,n}(k-1) \quad (30)$$

$$z_\ell(k) = z_\ell(k-1). \quad (31)$$

Consequently, the coefficient $\boldsymbol{h}_k$ is not updated either. Outside the mask interval, needless to say, the updating is performed according to Equations (21) and (22). This mask process can also be defined in a similar manner for LMS and RLS algorithms.

4. Numerical simulation

A reduction in the self-canceling components by implementing the proposed mask process is demonstrated in this section, with numerical examples.

4.1 Effects of mask process

Let us assume an environment where $f_0 = 50$[Hz] and $f_s = 1253$[Hz], as in Figure 2. In this example, the higher harmonic number is $m = 11$, and the reference signal is configured using components that are given by the respective parameters of Equation (1) as $A_0 \cdots A_{11} = 1, \theta_0 \cdots \theta_{11} = 0$. Furthermore, let the pulse-like signal, without any periodic interference added as shown in Figure 2(a), be $pls(k)$. The starting time thereof will be randomly assigned in intervals that are uniformly distributed in the range 488 to 512[ms]. Using the sequence $pls(k - \tau_i)$ that starts at time τ_i, $(i \in \{0, 1, \cdots, N_p\})$, we formed a desired signal as

$$s(k) = \sum_{i=0}^{N_p} pls(k - \tau_i). \quad (32)$$

Let the respective amplitudes of the cosine wave from Equation (2) be $G_0 = 0.33, G_1 \cdots G_3 = 0.06, G_4 \cdots G_6 = 0.03, G_7 \cdots G_9 = 0.012, G_{10} = G_{11} = 0.003$, and let the phase θ_i be given randomly within $(-\pi, \pi)$ to configure $n_{ac}(k)$. Furthermore, in anticipation of stochastic noise such as circuit noise that occurs while taking measurements, Gaussian white noise with standard deviation $\sigma = 0.0005$ is added to the main input $d(k)$. In order to evaluate the efficacy of the periodic interference cancellation, segments of 500[ms] are extracted from respective stimulus time points τ_i, with respect to $e(k)$ as follows:

$$pls\_est_i(k) = e(\tau_i + k), \quad \text{where} \quad k \in D = \{0, 1, \cdots, \lfloor 0.5 f_s \rfloor\}. \quad (33)$$

This is used to perform synchronous addition averaging:

$$\widehat{pls}(k) = \frac{1}{N_p + 1} \sum_{i=0}^{N_p} pls\_est_i(k). \quad (34)$$

Then the error

$$Err = \frac{\sqrt{\sum_{k \in D} \left(pls(k) - \widehat{pls}(k) \right)^2}}{\sqrt{\sum_{k \in D} pls^2(k)}} \quad (35)$$

is derived for comparison.

The errors (logarithmic representation) are shown for their respective methods, with regard to the number of synchronous addition averaging operations (logarithmic representation) in Figure 3. Figure 3(a) shows the result of performing synchronous addition averaging only (without performing periodic interference cancellation with an adaptive filter), which is labeled “simple average” in the diagram. Because the phase of the added periodic interference is random, the graph of the error fluctuates, but the amount decreases as the number of additions increases.

Figures 3(b), (c), and (d) are errors for cases where synchronous addition averaging is performed on the signal after canceling the periodic interference with an adaptive filter ($q = 23$) using Equations (15) and (20). The value of λ is 0.996, 0.999, and 0.9996, respectively, and the mask process has not been performed on any of these three examples. In cases where the number of synchronous addition averaging operations is low, the error is small in comparison to case (a),

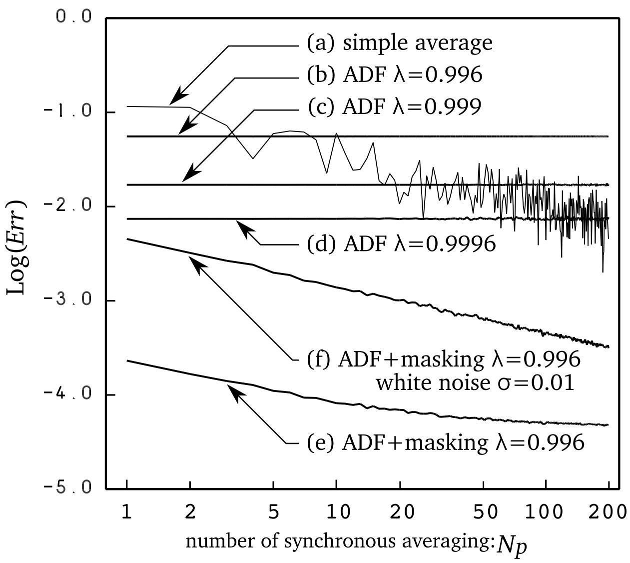

Fig. 3. Evaluation of mask process using the error

where no adaptive filter is used. However, this is reversed or becomes approximately equal within a few times in the case of (b), several tens of times with (c), and about 100 times with (d).

It is also evident that, even when the number of synchronous addition averaging operations is increased, absolutely no change takes place. This signifies that the magnitudes of the self-canceling components depend only on the pulse-like signal and the size of λ, and are unrelated to the periodic interference.

The error due to the self-canceling components decreases as λ approaches 1, but there are various restrictions, depending on the fields of application. For this sampling frequency and $\lambda = 0.9996$, the adaptation time to keep the past influence to 1% or lower is about 9[s]. In actual ERG tests, it would not be desirable to set the adaptation time longer than this, as described at the beginning of Section 3.

On the other hand, the example with λ set to 0.996 and the mask process implemented for 200[ms] (the " ADF+masking " shown in the diagram) is (e), which has an extremely small amount of error in comparison to (a) with respect to all the number of synchronous averaging operations. The effectiveness of the approach used in this example is clear.

4.2 Influence of stochastic noise and mask length

In the previous section, errors were evaluated by adding a Gaussian white noise of $\sigma = 0.0005$ to the main input signal, in order to simulate the stochastic noise. However, there are cases where an even larger stochastic noise is added.

Adaptive filters that do not perform the mask process output stochastic signal with respect to the stochastic components included in the desired signal $s(k)$, because Equation (27) is a linear filter for $s(k)$. This means that the synchronous addition averaging process can decrease the magnitude of the stochastic components even if the process has any synchronous timing. In this case, consequently, no problems arise. On the other hand, it is necessary to verify that the mask process does not result in the generation of components that cannot be reduced even by using the synchronous addition averaging process.

The error given by Equation (35) for cases where the mask process is performed is composed of two types of components:

(A) Periodic interference components arising from a deterioration in the accuracy of estimating the filter coefficient. This is because of stochastic noise that occurred immediately prior to the generation of the pulse-like signal (immediately before the mask process).

(B) Components of the stochastic noise itself, which are added to the main input.

It is possible to reduce (B) by performing the synchronous addition averaging process, using any timing, based on the aforementioned considerations. It is also presumed that with (A), the periodic interference will decrease as the number of synchronous addition averaging operations increases. The reason is that the influence of the pulse-like signal is not reflected in the estimation of the filter coefficient because, from the causality, there is no component in the stochastic noise that correlates to the pulse-like signal.

Figure 3(f) shows the change in the error for the case where only the standard deviation of the Gaussian white noise, added to $d(k)$ under the same condition as (e) of the same figure, is set to $\sigma = 0.01$. The error decreases linearly as the number of synchronous addition averaging operations increases. This agrees with the prediction described earlier. Because the reference signal is the periodic interference, a mask process has no cancellation effect on the stochastic noise. However it does not inhibit the essential performance of the synchronous addition averaging. Therefore, both the mask process and the synchronous addition averaging can be used together.

Furthermore, cases where the mask cannot completely cover the signal may be anticipated in applications where the sustained time of the pulse-like signal is not known in advance, or where the sustained time may vary for each measurement. In such a situation, the error due to the self-canceling components is expected to decrease as the mask length is increased. In other words, it is desirable to have the best results for the length of the mask, even if the mask length was not sufficient. That is, a monotonic decrease in the error is expected with respect to the increase in mask length.

When the error of stochastic noise becomes larger than that of the self-cancelling components, the effect of the mask process will be overcome by stochastic noise. Consequently, there would exist a certain length such that a larger mask than the length has no effect in terms of the error, in the situation where the monotonicity mentioned earlier exists. This also means that it is possible to determine an adequate mask length depending on the levels of a given stochastic noise from the stand point of implementation.

Figure 4(a) shows the error from a case where synchronous addition averaging is performed on the result of ten instances of periodic interference cancellation ($\lambda = 0.996$) for any mask length. A standard deviation of the added Gaussian white noise of $\sigma = 0.0005$ is used, and the mask length varies from

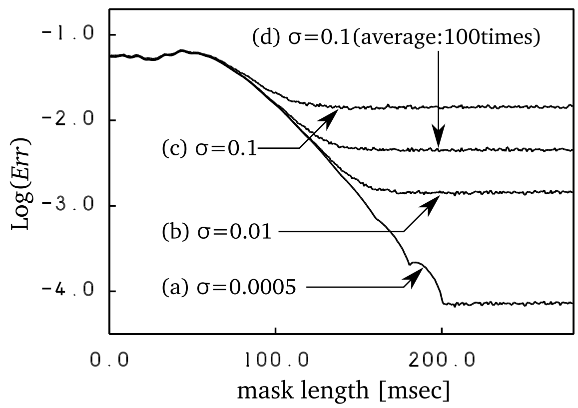

Fig. 4. Error versus mask length and magnitude of stochastic noise

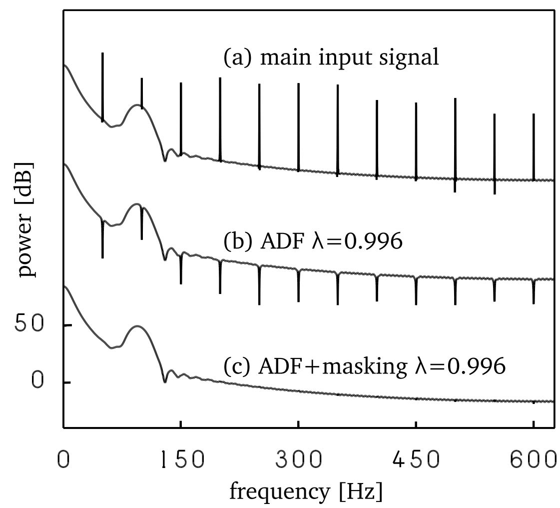

Fig. 5. Effects of the mask process appeared on the spectra

0 to 300[ms]. The change in error can be considered to be practically monotonic and smooth.

The results of cases where the standard deviation of the stochastic noise is amplified to $\sigma = 0.01$ and $\sigma = 0.1$ are shown in Figures 4(b) and (c), respectively. In cases where the mask is short, all graphs overlap, but the lower limit for the error that can be achieved has higher values when the stochastic noise is larger. On each graph, we observe that there exists a minimum mask length such that no change in error occurs. Consequently, such a minimum mask length would be considered appropriate. Furthermore, Figure 4(d) shows the error for the case where σ is set to 0.1 and the number of synchronous addition averaging operations is set to 100 (labeled "average: 100 times" in the figure). It is evident that, by using a longer mask by increasing the number of synchronous addition averaging operations, it is possible to reduce the noise further than the reduction shown in Figure 4(c), whose stochastic noise has the same magnitude.

This suggests that the effect can be improved with long masks when the stochastic noise is low and a large number of synchronous addition averaging operation is performed. Depending on the properties of the stochastic noise, however, it is conceivable that there would be cases where having the filter coefficient for sufficiently canceling the periodic interference immediately before the implementation of the mask (as described at the beginning of Section 3) is not satisfied. Further investigation is required to shed light on this aspect, including issues relating to the actual determination of mask lengths.

4.3 Verification on spectrum

The effectiveness of periodic interference cancellation in the frequency domain in cases where the number of synchronous addition averaging operations is set to one (no averaging performed) is verified for the various methods here. In order to ensure that the effect can be seen clearly, no stochastic noise is added to the main input signal $d(k)$ given in Subsection 4.1. Figure 5(a) shows the power spectrum of $d(k)$ for the case where an adaptive filter is not used. It is evident that 12 sharp peaks that indicate periodic interference are manifested on the wide distribution of the essential frequency components of the pulse-like signal. It can be verified that the self-canceling components manifest as notches in the periodic interference frequency in spectrum (b), which occurs when the periodic interference cancellation process is performed with an adaptive filter ($\lambda = 0.996$, $q = 23$) without performing any mask processing on the signal. What is shown in (c), on the other hand, is the spectrum resulting from the cancellation performed using an adaptive filter that has the same λ and q, but with the proposed mask process implemented. No notch or peak is confirmed in this instance.

5. Application to actual ERG

In this section we demonstrate the effective functioning of an adaptive filter using the proposed mask process, with an actual measurement test of ERG using flash light stimuli.

Flash light ERG (also referred simply to as flash ERG), with eyes adapted to the darkness, is a pulse-like signal that exhibits a rapid change in potential in the negative direction a few milliseconds after the stimulus (a-wave). This is followed by a relatively gradual change to the positive direction (b-wave), and four to six waves of small oscillatory potential (OP) overlapping these waves[3]. The magnitude of the respective components varies depending on the intensity of the flash light stimulus, but the overall duration is generally approximately 200 to 300[ms]. The amplitude is up to several hundred μV_{p-p} on the cornea, while on the skin of the lower eyelid it is even lower (only a fraction thereof).

Thus, the ERG signal is a minute electric potential. In addition, periodic interference arises from the commercial alternating-current power source, as well as brain-waves, myoelectric, and cardiographic signals, and other biosignals. These are all added to the measured values as noise. For these reasons, the synchronous addition averaging process for multiple flash light stimuli is ordinarily performed with an ERG test.

In this instance, however, we verify a case of a single instance of the ERG (without the synchronous addition averaging) in order to emphasize the effectiveness of the mask

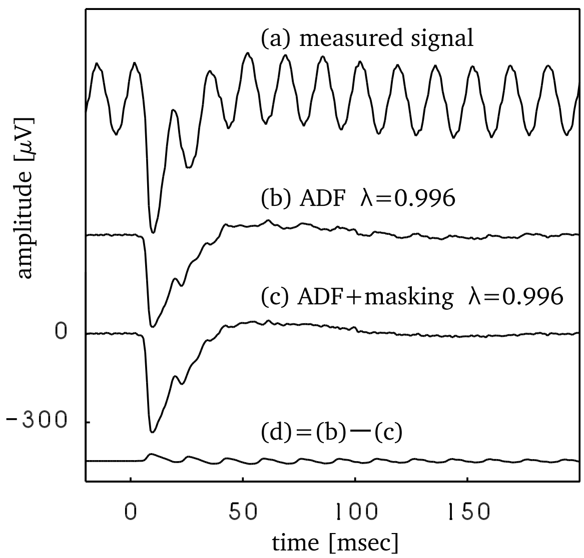

Fig. 6. Application to an actual flash ERGs

process.

Figure 6(a) shows the measurement of the response potential (labeled "measured signal" on the diagram) with respect to the strong flash light stimulus (time: 0[ms]) with eyes adapted to the darkness. A contact-lens-type electrode was fitted on the cornea of a male in his fifties, in an environment where a significant amount of periodic interference (fundamental frequency of 60[Hz]) exists. Records of measurements were taken at a sampling frequency of $f_s = 1253$[Hz], after implementing a low-pass filter (cutoff frequency of 500[Hz] and attenuation factor of -80[dB/Oct]). The ERG could not be verified because it was covered by the periodic interference of larger amplitudes. The spectrum of the signal (periodogram) with $16,384$ points, which includes the response interval of the ERG, is shown in Figure 7(a). The periodic interference is manifested prominently as a component with acute lines at a frequency of 60[Hz], as well as odd multiples thereof. This is considered to be the main input $d(k)$.

Furthermore, the signal acquired directly from the commercial alternating-current power source turned into a short pulse through analog means at the zero cross-point from negative to positive. The direct-current portion was canceled, and a low-pass filter with the same characteristics as the main input was applied and then sampled as the reference signal $u(k)$. Figure 7(b) shows its spectrum. A small number of peaks due to aliasing was confirmed, but the components of the fundamental frequency and the higher harmonic wave had amplitudes that exceeded 70[dB] from the upper section of the continuous spectrum of circuit noise, and were approximately equal.

The result of canceling the periodic interference from $d(k)$ and $u(k)$ by using an adaptive filter ($q = 21$, $\lambda = 0.996$) of Equations (15) and (20) is shown in Figure 6(b). The periodic interference was canceled to the extent that the a-wave, b-wave, and the oscillatory potential can be verified. Although this effect is considered substantial, it was confirmed that the vibrational components persist for a long time after the response. On the basis of the way they are presented, it is difficult to determine whether these vibrational components are part of the ERG or are other noises. Because notches are confirmed at 60[Hz] and 120[Hz] in the spectrum of this signal (Figure 7(c)), the vibrational components are believed to be self-canceling components due to the ERG.

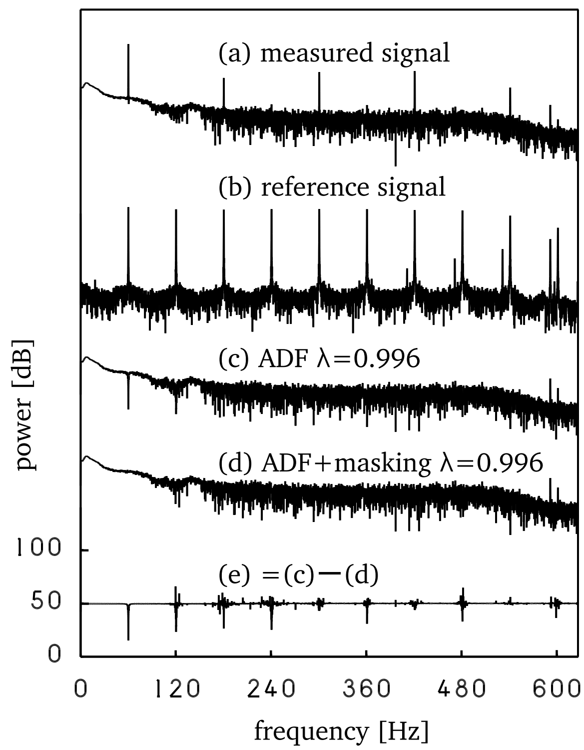

Fig. 7. Spectra of signals appeared in processing the actual ERGs

This example of the ERG indicates that the interval in which a rapid change occurs practically ends 200[ms] after the flash light stimulus. It is difficult to believe that the characteristics of the periodic interference changed during this interval. An attempt was made here to cancel the periodic interference with an adaptive filter ($\lambda = 0.996$) having a mask interval at the time point of 200[ms] from the flash light stimulus pulse emission. Figure 6(c) shows the results, and reveals that the vibration components that existed in (b) of the same figure had disappeared.

In order to clarify this point, a signal derived by subtracting (c) from the signal of (b) is shown in (d) of the same figure. Figure 6(d) shows the extraction of the vibration with a fundamental frequency of 60[Hz] that appears from where the ERG starts. This can be considered the self-canceling components that were extracted and canceled by the proposed mask process. No notch could be confirmed on the spectrum (Figure 7(d)) of the signal that resulted from the implementation of the mask process (Figure 6(c)). In order to clarify this even further, the spectrum of (d) was subtracted from that of (c) as well, and shown in (e). It was possible to verify that notches existed on the spectrum of (c), even on harmonic waves of 180[Hz] and higher. This revealed that the self-canceling components had been canceled effectively.

6. Conclusions

The existence of self-canceling components triggered by a desired signal was demonstrated from a theoretical perspective. This was based on the formula of the successive least squares method, a fundamental format of the adaptive algorithm, which was used to cancel periodic interference by using an adaptive filter. This paper clarified the danger of the error due to the self-canceling components becoming larger with a larger number of synchronous addition averaging operations (compared to instances when the adaptive filter is not used) in cases where the desired signal is a pulse-like signal. A mask process, which involved no updating correlations and filter coefficients in intervals where the pulse-like signal persisted, was proposed. The effective cancellation of the self-canceling components was verified through a numerical simulation, as well as with an ERG that was actually measured.

Furthermore, the mask process does not degrade the synchronous addition averaging process, even when stochastic noise is included, and hence the combined use of these two processes is possible. Because the error decreases monotonically as the mask is extended, it was confirmed that the effectiveness of the mask process increases in environments where a larger number of synchronous addition averaging operations can be performed and the stochastic noise is small. Analyses from a theoretical perspective, as well as determination of the mask length, are necessary to clarify these aspects.

The ERG was utilized as an application example of the mask process in this paper, but applications can be considered for a variety of other fields. In the analyses of evoked potentials, for example, the existence of periodic interference is believed to affect the estimation of wave parameters [18], and the proposed method is considered to be applicable. The proposed method is also expected to be in the measurement of impulse responses, such as in communication systems.

Periodic interference arising from the display units of information equipment, as well as rotating machinery such as pumps, has frequencies that are different from those of commercial power sources. In such cases, although acquiring reference signals would be difficult, adaptive filters can be used by generating an alternative reference signal based on an appropriate frequency analysis of periodic interference included in the main input signal only. Even in such cases, self-canceling components may be generated, and using the proposed mask process can be expected to improve performance.

The mask process, on the other hand, cannot be used when the pulse-like signal occurs frequently or when the desired signal is stochastic. In the ERG test, for example, the test referred to as “flicker,” whose stimuli consist of a flash light train with a high frequency, is performed. When the mask process is applied in such cases, the masks overlap each other while the stimuli continue, and no updating will be performed. This makes tracking the changes to the characteristics of the periodic interference inconvenient or infeasible. The same is true for sustained stochastic signals, such as EEG or myoelectricity. In the future, it will be necessary to consider methods that do not involve the mask process for such signals.

Acknowledgments

Ms. Maiko Tsutsui of Chuden CTI Co., Ltd. provided assistance with the data analysis in this paper while she was attending our institution. Furthermore, Mr. Masao Yoshikawa, Mr. Eiichiro Nagasaka, and Mr. Hidetaka Kudo of Mayo Corporation provided critical data and advice. The method proposed by this paper has been adopted as a part of the AC noise-canceling engine PURE (PUlse REference power line noise reduction) mounted on the evoked response recorder PuREC (certification number: 221AGBZX00232000) that is manufactured by Mayo Corporation. I would like to express my gratitude to everyone who assisted with this paper.

References

[1] N.Hoshimiya, Biological Information Measurements (in Japanese), Morikita Publishing, 1997.

[2] K. Suenaga and Y. Okada, Standard Brainwave Text, NEC Medical Systems Training Center, 1998.

[3] I. Watanabe and Y. Miyake, Clinical ERG and EOG, Igaku-Shoin, 1984.

[4] J.V. Odom, M. Bach, C. Barber, M. Brigell, M.F. Marmor, A.P. Tormene, G.E. Holder and Vaegan, “Visual evoked potentials standard (2004), ” Documenta Ophthalmologica vol.108, pp.115–123, 2004.

[5] S.P. Meredith, M.A. Reddy, L.E. Allen, A.T. Moore and K. Bradshaw, “Full-field ERG responses recorded with skin electrodes in paediatric patients with retinal dystrophy,” Documenta Ophthalmologica, vol.109, pp.57–66, 2004.

[6] Y. Miyake, “ Fovial area localized ERG, ” Ganka MOOK, no. 41, pp. 110—123, 1989.

[7] H. Kato and N.Toda,“A Method for Elimination of Alternative Noise by Digital Control of an Analog Laguerre Filter in Biopotential Mesurements,” Systems and Computers in Japan, vol.36, no.14, pp.1-10, 2005.

[8] A.C. Fisher, A.F.G. Taktak, R.P. Hagan, and M.C. Brown, “Automated post hoc removal of power-line and CRT frame pulse contamination from retinal and cortical evoked potentials,” Documenta Ophthalmologica, vol.112, pp.169-175, 2006.

[9] B. Widrow, J.R. Glover Jr., J.M. McCool, J. Kaunitz, C.S. Williams, R.H. Hearn, J.R. Zeidler, E. Dong Jr. and R.C. Goodlin, “Adaptive noise cancelling: principles and applications,” Proc.IEEE, vol.63, pp.1692-1716, 1975.

[10] J.R. Glover Jr., “Adaptive noise canceling applied to sinusoidal interferences,” IEEE Transactions on Acoustics, Speech and Signal Processing, vol.25, no.6, pp.484–491, 1977.

[11] S. Heikin (author); H. Suzuki, K. Hankawa, T. Ogane, J. Takada, H. Murata, and Y.Sanada (translators); S.O. Haykin, Adaptive Filter Theory, Kagaku Gijutsu Shuppan, 2000.

[12] M. Umayahara, Y. Iiguni and H. Maeda, “A Nonlinear Rcursive Least Square Algorithm for Crosstalk Resistant Noise Canceller,” IEICE Transactions on Fundamentals of Electronics, Communications and Computer Sciences A, vol.85-A, no.2, pp.162–169, 2002.

[13] M.J. Shensa, “Non-Wiener solution of the adaptive noise canceller with a noisy reference” IEEE Transactions on Acoustics, Speech and Signal Processing, vol.28, no.4, pp.468–473, 1980.

[14] N.J. Bershad and J.C.M. Bermudez, “Sinusoidal interference rejection analysis of an LMS adaptive feedforward controller with a noisy periodic reference,” IEEE Transactions on Signal Processing, vol.46, no.5, pp.1298–1313, 1998.

[15] Y.Z. Ider and H. Koymen, “A new technique for line interference monitoring and reduction in biopotential amplifiers,” IEEE Transactions Biomedical Engineerring, vol.31, no.6, pp.624–631, 1990.

[16] C. Levkov, G. Mihov, R. Ivanov, I. Daskalov,I. Christov and I. Dotsinsky, "Removal of power-line interference from the ECG: A review of the subtraction procedure," BioMedical Engineering OnLine 2005, 4:50, 2005.

[17] S.M.M. Martens, M. Mischi, S.G. Oei and J.W.M. Bergmans, "An improved adaptive power line interference canceller for electrocardiography," IEEE Transactions on Biomedical Engineering, vol.53, no.11, pp.2220–2231, 2006.

[18] S.D.Georgiadis, P.O.Ranta-aho, M.P.Tarvainen and P.A.Karjalainen, "A Subspace Method for Dynamical Estimation of Evoked Potentials," Computational Intelligence and Neuroscience, vol.2007, Article ID 61916, 11 pages, 2007.

APPENDIX
DERIVATION OF EQUATION (27)

Consider the individual elements of Equation (15). First, $r_{0,0}(k)$ of $\boldsymbol{R}_k$ is derived by

$$\begin{aligned} r_{0,0}(k) &= \sum_{i=0}^{\infty} \lambda^i \cos^2(f(k-i)) \\ &= \sum_{i=0}^{\infty} \lambda^i \left(\frac{1}{2} \left(e^{jfk} e^{-jfi} + e^{-jfk} e^{jfi} \right) \right)^2 \\ &= \frac{1}{2} \sum_{i=0}^{\infty} \lambda^i + \frac{e^{j2fk}}{4} \sum_{i=0}^{\infty} \lambda^i e^{-j2fi} \\ &\qquad + \frac{e^{-j2fk}}{4} \sum_{i=0}^{\infty} \lambda^i e^{j2fi} \\ &= \frac{1}{2(1-\lambda)} + \frac{e^{j2fk}}{4(1-\lambda e^{-j2f})} + \frac{e^{-j2fk}}{4(1-\lambda e^{j2f})} \\ &= \frac{1}{2(1-\lambda)} + \frac{\cos(2fk) - \lambda \cos(2f(k+1))}{2(1-2\lambda\cos(2f)+\lambda^2)} \\ &= \frac{1}{2(1-\lambda)} + \frac{\cos(2fk) - \lambda \cos(2f(k+1))}{2((\lambda - \cos(2f))^2 + \sin^2(2f))}. \end{aligned} \quad (A\cdot1)$$

Considering a situation where λ approaches 1, the second term on the right side is $f \neq \ell\pi$, $(\ell \in \{0, \pm1, \pm2, \cdots\})$, and is therefore finite, whereas the first term increases without limit, and the following approximation holds:

$$r_{0,0}(k) \approx \frac{1}{2(1-\lambda)}. \quad (A\cdot2)$$

Similarly, we have the following approximations:

$$\begin{aligned} r_{0,1}(k) &= r_{1,0}(k) \\ &= \sum_{i=0}^{\infty} \lambda^i \cos(f(k-i)) \cos(f(k-1-i)) \\ &= \frac{\cos f}{2(1-\lambda)} + \frac{\cos(f(2k-1)) - \lambda \cos(f(2k+1))}{2(1-2\lambda\cos(2f)+\lambda^2)} \\ &\approx \frac{\cos f}{2(1-\lambda)} \end{aligned} \quad (A\cdot3)$$

$$\begin{aligned} r_{1,1}(k) &= \sum_{i=0}^{\infty} \lambda^i \cos(f(k-1-i)) \cos(f(k-1-i)) \\ &= \frac{1}{2(1-\lambda)} + \frac{\cos(2f(k-1)) - \lambda \cos(2fk)}{2(1-2\lambda\cos(2f)+\lambda^2)} \\ &\approx \frac{1}{2(1-\lambda)}. \end{aligned} \quad (A\cdot4)$$

Using $\delta(i)$ defined by Equation (23), Equation (26) can be expressed as

$$d(k) = s(k) = \sum_{\tau=0}^{\infty} s(\tau)\delta(k-\tau). \quad (A\cdot5)$$

Thus the respective elements of z_k on the right-hand side will be

$$\begin{aligned} z_0(k) &= \sum_{i=0}^{\infty} \lambda^i \Big(\sum_{\tau=0}^{\infty} s(\tau)\delta(k-\tau-i) \Big) \cos(f(k-i)) \\ &= \sum_{\tau=0}^{\infty} s(\tau) \lambda^{k-\tau} \cos(f\tau) \end{aligned} \quad (A\cdot6)$$

$$\begin{aligned} z_1(k) &= \sum_{i=0}^{\infty} \lambda^i \Big(\sum_{\tau=0}^{\infty} s(\tau)\delta(k-\tau-i) \Big) \cos(f(k-1-i)) \\ &= \sum_{\tau=0}^{\infty} s(\tau) \lambda^{k-\tau} \cos(f(\tau-1)). \end{aligned} \quad (A\cdot7)$$

Using these results, and by solving Equation (15), the approximation solution of the filter coefficients $h_0(k), h_1(k)$ are given as

$$\begin{aligned} \widetilde{h_0}(k) &= \sum_{\tau=0}^{\infty} s(\tau) \frac{2(1-\lambda)}{1-\cos^2 f} \lambda^{k-\tau} \Big(\cos(f\tau) \\ &\quad - \cos f \cos(f(\tau-1)) \Big) \end{aligned} \quad (A\cdot8)$$

$$\begin{aligned} \widetilde{h_1}(k) &= \sum_{\tau=0}^{\infty} s(\tau) \frac{2(1-\lambda)}{1-\cos^2 f} \lambda^{k-\tau} \Big(-\cos f \cos(f\tau) \\ &\quad + \cos(f(\tau-1)) \Big). \end{aligned} \quad (A\cdot9)$$

The approximation solution for the filter output given by Equation (4), therefore, becomes

$$\begin{aligned} \widetilde{y}(k) &= \widetilde{h_0}(k)\cos(fk) + \widetilde{h_1}(k)\cos(f(k-1)) \\ &= \sum_{\tau=0}^{\infty} s(\tau) 2(1-\lambda) \lambda^{k-\tau} \cos(f(k-\tau)). \end{aligned} \quad (A\cdot10)$$

Naohiro Toda Completed the doctoral program in engineering and received the Doctor of Engineering degree from the Graduate School of Toyohashi University of Technology in 1990. He was appointed to the post of Assistant Professor in Information Engineering at the university. In 1992, he was appointed to the post of Lecturer in Electrical Engineering at Maizuru National College of Technology, and in 1994, he was appointed to the post of Lecturer in Information Engineering at Toyohashi University of Technology. He also served as Visiting Researcher at the University of Southern California in 1995. In 1999, he was appointed to the post of Associate Professor and in 2002 to the post of Professor at the Department of Information Science and Technology of Aichi Prefectural University. His research interests are medical imaging, signal processing, and nonlinear time series analysis. He is a full member of IEEE and the Society of Instrument and Control Engineers.